A complete Simulation and investigation of the hood's airflow under Isothermal suction conditions using CFD

Yadolla Nowrouzi Moghaddam[1], Sadegh Abbasnia [2,] *

[1]Islamic Azad University, Shiraz Branch, Department of Mechanical Engineering, Sadra Town Road, P.O. Box 1-71991, Shiraz, Iran

[2] Iranian Research Organization for Science and Technology (IROST), Department of Chemical Technologies, Azadegan Highway, P.O. Box 33535111, Tehran, Iran

Corresponding author E-mail address: ***sadeghabbasnia@chmail.ir***

Abstract

In this study, the range of influence of industrial hoods under isothermal conditions has been investigated. For the investigation, a control volume with certain dimensions has been considered around the hood. The suction velocity at the center of the hood is 20 m/s, and to simulate the real state, the side walls have been considered as air inlets at atmospheric pressure. The hood suction has been analyzed for distances of 1, 1.5, 2, 2.5, and 3 m from the floor. Geometry generation, meshing, and numerical solution of the problem have been performed using ANSYS-FLUENT software. To analyze the flow field, the Navier-Stokes and continuity equations have been solved using the turbulent k-ε model. The effect of the hood opening dimensions, the hood distance from the floor, and its suction velocity in different cases has been investigated. The velocity diagram on an imaginary line from the hood center to the floor, as well as the velocity and pressure contours for different distances, have been extracted and investigated. The capture zone was analyzed for each of the mentioned distances, and it was determined that the hood's capture zone at a distance of 2 meters from the floor was the best possible.

Keywords: Hood, Capture zone, K-ε Turbulent Model, Velocity and Pressure Contour

1. Introduction

In recent years, many studies have been conducted on industrial hoods and their optimization. The ACGIH report [1] showed that properly designed industrial hoods can control up to 90 percent of pollutants. Flynn and Lj [2] emphasized that the flow rate and the distance of the hood from the source of pollution play a key role in the suction efficiency. These findings indicate the need to use

numerical simulation to improve the performance of hoods. Lander and Spalding [3] first introduced the standard k-ε model to simulate flows around hoods. However, this model has limitations in flow separation regions. Wilcox [4] improved the accuracy of the K-ε model in complex flows by adjusting the C1 coefficient and enhancing its prediction of rotational stresses. Zhang and Chen [5] showed with CFD that precise mesh simulation provides more accurate results than experimental methods. Safarzadeh and colleagues [6] warned that excessive negative pressure (-1100 pa) can increase the dispersion of pollutants. Wang et al. [7] attributed the unexpected increase in velocities to the heterogeneity of inlet conditions or flow separation. They suggested that careful meshing could mitigate this problem. Zhao et al. [8] investigated the effects of different hood shapes, side panels, and exhaust duct arrangements on the performance of conventional Chinese-style range hoods. In this study, various types of hood shapes and side panels were studied to improve the absorption efficiency of traditional Chinese range hoods. The exhaust duct arrangement was also investigated. The simulated results showed that increasing the hood volume did not improve the absorption performance. However, the side panels improved the efficiency, especially at higher positions. In addition, when the exhaust port was located at the back of the hood, the improvement in the absorption efficiency of the hood was further enhanced. Huang and colleagues [9] conducted four case studies to investigate industrial ventilation guidelines for smoke and dust control. The first case found that building hoods with large aspect ratios could improve the suction rate. The second case looked at the precise characteristics of dust generated from bulk material handling. The results showed that the dust emission rate could be reduced by reducing the drop height and the dust diameter. The third and fourth cases were about water and fluid pollution. These studies provide valuable results for the development of high-efficiency ventilation systems with improved indoor air quality and low energy consumption for industrial buildings. Logachev et al. [10] investigated the dynamics of dust around a conical hood under high flow conditions. They used the discrete vortex method to simulate the moving fluid, separating the flow at the sharp edges of the conical hood. To evaluate the collection efficiency, they numerically determined the suction coefficient using the limiting paths drawn for the dust particles. They used the rules of previous researchers to validate their findings. Using the rules they discovered, the hood design can be adjusted for a variety of application conditions in terms of dust collection efficiency. Logachev and colleagues [11] studied the outlines of the vortex zones that occur at the hood inlet. They wrote a mathematical model and a computer program to calculate the velocity fields at the boundaries of

the vortex zones. They concluded that shaping the vortex lines with an inclination angle of ninety degrees makes it possible to reduce the local drag coefficient by more than ten times. Zhang and colleagues [12] investigated the critical velocity when using an air jet to increase the opening of a rectangular hood. This paper proposes a new type of advanced hood with a rectangular opening instead of a circular opening. Kim and Lee [13] emphasized the importance of validating simulation results with ACGIG standards. Yang Liu and colleagues [14] conducted simulations and experiments on three types of conventional exhaust hoods, side exhaust hoods, and air curtains. They concluded that these hoods differ significantly in efficiency, with the conventional exhaust hood having the lowest efficiency and the air curtains having the highest efficiency. This research has an important innovation in the study of dust collection mechanisms and provides strong theoretical and experimental support for innovations. Li et al. [15] investigated the use of air curtain hoods for dust collection in a tobacco factory. In this study, the problem of dust leakage at the stem loading point was addressed. The results showed that when the main hood was working, the dust collection efficiency was 16.35%, indicating serious dust leakage. After using the air curtain hood system, the efficiency reached 94.76%. Their experimental results validated the better application effect of the developed air curtain dust collection system compared with the main dust collection system at the industrial loading point. Logachev et al. [16] demonstrated the reduction of pressure drop in a circular exhaust hood. They experimentally determined the local drag coefficient of a circular hood. They performed the measurement using two methods. In the first method, they measured the drag coefficient with and without friction using a micronanometer. In the second method, they determined the velocity and pressure distribution in a boundary layer with pressure miniprobes. The results of their work showed that by shaping the hood inlet edges, a drag reduction of more than 90% could be achieved. This increased the range of pollutant absorption and prevented the pollutants from leaving the hood by eliminating vortex zones and reducing fan power. Song et al. [17] investigated the control of kitchen pollutants by exhaust hoods with air-filled gaps. This paper proposes a method of air conditioning the kitchen exhaust system to improve the hood performance by creating an air curtain between the stove and the hood. In this paper, numerical simulations are performed to compare the conditions with air-filled gaps and without active conditioning conditions. This research establishes the optimal operating conditions of the air unit of the island exhaust hood and improves the organization of the kitchen airflow. In

the works of [18,19,20,21,22,23,24], complete studies have been conducted via CFD on the liquid and gas phases by various models.

2. Simulation

In this study, a turbulent air flow around the hood was simulated using the k-ε turbulence model, and the effect of the hood distance from the floor (1, 1.5, 2, 2.5, and 3 meters) on the suction effect range and velocity distribution in the hood centerline was studied. The velocity and pressure profile around the hood was analyzed, and the area where the flow velocity exceeds the standard thresholds was extracted. The flow line pattern and capture zone were examined, and the changes in this area were determined at different hood distances. Given that in this study, the range of effect of hoods at distances of 1 to 3 meters from the floor is investigated, the numerical simulation results can be compared with the criteria proposed by ACGIH. (American Conference of Governmental Industrial Hygienists) Therefore, if the flow rate at different points is lower than the standard values of this organization, the hood's efficiency in collecting pollutants is insufficient, and necessary modifications should be made in the design (increasing the flow rate, changing the dimensions, or reducing the distance of the hood from the source).

2.1. Simulation conditions

1-The working fluid is considered to be air, whose properties are constant and independent of temperature.

2-The air flow is assumed to be incompressible. (The air density does not change along the flow range)

3-The flow regime is turbulent.

4-The steady flow is considered to be isothermal (constant temperature).

5-The boundary conditions of the ambient pressure are atmospheric, and the air suction is done only by the hood.

6-The hood is simulated with dimensions of 1.5 × 0.65 m.

7-The inlet velocity at the hood opening is constant and equal to 20 m/s.

8-The walls are assumed to be rigid and impenetrable, and the effect of surface roughness is ignored.

9-The effect of gravity and thermal buoyancy forces is not considered in this study.

10-Different distances of the hood from the floor of 1, 1.5, 2, 2.5, and 3 meters are considered as the main parameters of the study.

2.2. Equations

2.2.1. Continuity Equation

For an incompressible fluid:

$$\partial \rho/\partial t + \nabla \cdot (\rho\, u) = 0 \quad (1)$$

Where **ρ** is the fluid density (kg/m³), **t** is the time (s), and **u** is the fluid velocity vector (m/s).

2.2.2. Momentum equations (Navier–Stokes)

$$\partial\, (\rho\, u)/\partial t + \nabla\cdot\, (\rho\, u\, u) = -\nabla p + \nabla\cdot\tau + \rho\, g + F \quad (2)$$

$$\tau = \mu\, (\nabla u + (\nabla u)^{T}) - 2/3\, \mu\, (\nabla\cdot u)\, I \quad (3)$$

Where **p** is pressure (Pa), **τ** is the shear stress tensor, **g** is the gravitational acceleration (m/s²), **F** is the other volumetric forces (N/m³), **μ** is the dynamic viscosity (Pa·s), and **I** represents the conservation of momentum and the effect of pressure, viscosity, and external forces.

2.2.3. Turbulence equations

$$\partial\, (\rho\, k)/\partial t + \nabla\cdot\, (\rho\, u\, k) = \nabla\cdot\, [(\mu + \mu\_t/\sigma\_k)\, \nabla k] + P\_k - \rho\, \varepsilon \quad (4)$$

$$\partial(\rho\, \varepsilon)/\partial t + \nabla\cdot(\rho\, u\, \varepsilon) = \nabla\cdot[(\mu + \mu\_t/\sigma\_\varepsilon)\, \nabla\varepsilon] + C_{1\varepsilon}\, \varepsilon/k.\, P\_k - C_{2\varepsilon}\, \rho\, \varepsilon^2/k \quad (5)$$

$$\mu\_t = \rho\, C\_\mu.\, k^2/\varepsilon \quad (6)$$

k is the kinetic energy of turbulence (m²/s²), **ε** is the rate of turbulence dissipation (m²/s³), **μ_t** is the viscosity of turbulence (Pa·s), **σ_k**, **σ_ε**, $\mathbf{C_{1\varepsilon}}$, $\mathbf{C_{2\varepsilon}}$, and **C_μ** are the coefficients of the model. **k-ε** and **P_k** of the production of kinetic energy of turbulence.

2.3. Geometry and meshing

First, in the geometry space of the software, a hood with dimensions of 1.95 × 0.65 meters is planned, and a space measuring 1.5 × 3 × 1.3 meters (the distance from the hood to the floor is 1 meter) is planned around it as a control volume. Figure 1 illustrates the geometry of the planned hood and the control volume. Figure 2 depicts the meshing of the planned hood and the control volume.

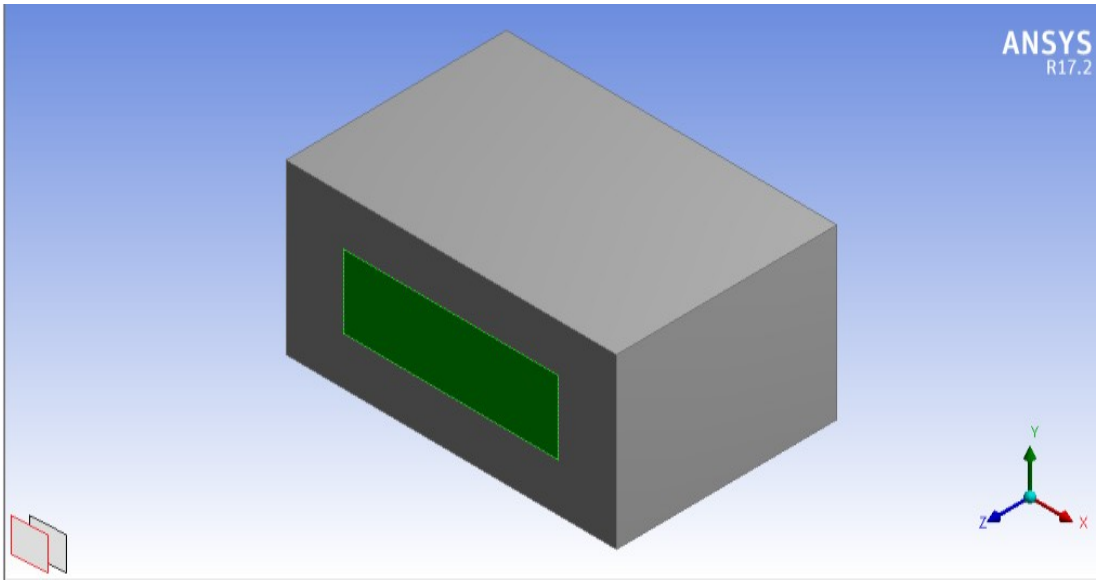

Figure 1: The geometric shape of the hood

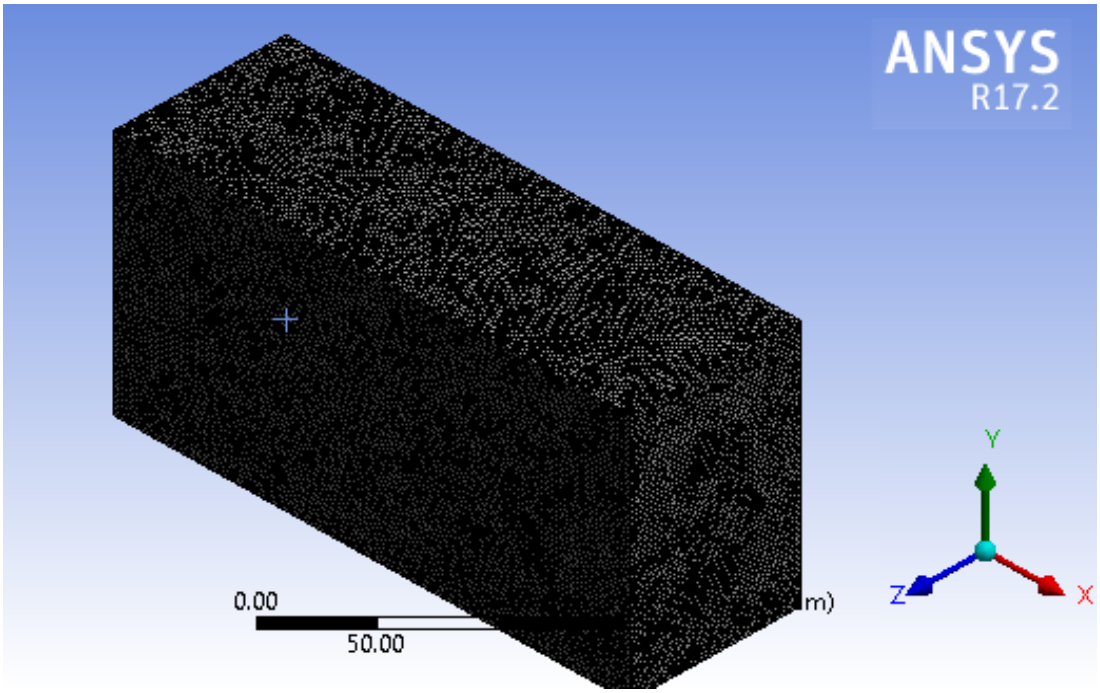

Figure 2: The meshing shape of the hood

3. Results

3.1. Velocity and pressure contours

Figure 3 illustrates 2 planes (blue and red) for examining pressure and velocity contours. The unit of velocity in the velocity contours is m/s, and the unit of pressure in the pressure contours is Pa.

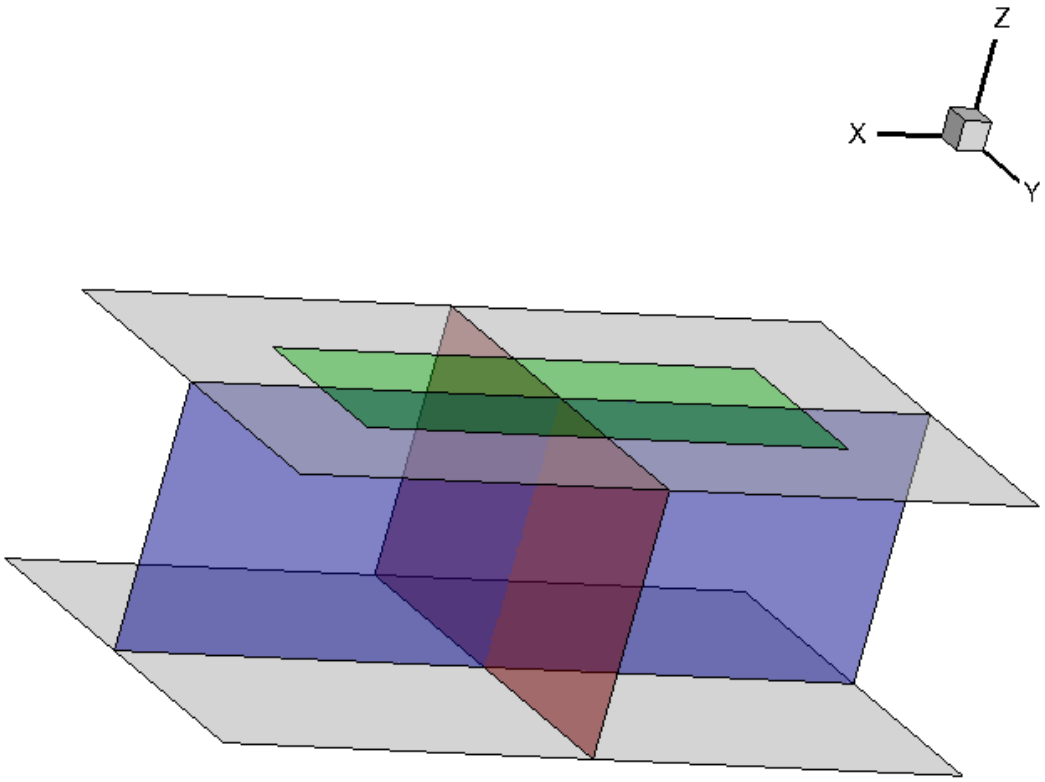

Figure 3: 2 plates for examining contours

3.1.1. Velocity and pressure contours when the hood is at a distance of 1 meter from the bottom

In Figure 4a, as can be seen in the velocity contour on the x-z plane for a distance of 1 m, the velocity starts from 20 m/s at the hood inlet and decreases rapidly, which is due to the proximity to the bottom and the strong wall effect. The velocity gradient in the x-z plane is very steep, indicating flow disturbance and vortex formation near the bottom.

Figure 4b shows the pressure distribution on the x-z plane. The negative pressure starts at the hood inlet and quickly approaches atmospheric pressure, which is a rapid change due to weak suction. The pressure gradient in the plane is steep, indicating flow disruption and pressure increase near the bottom due to the wall effect.

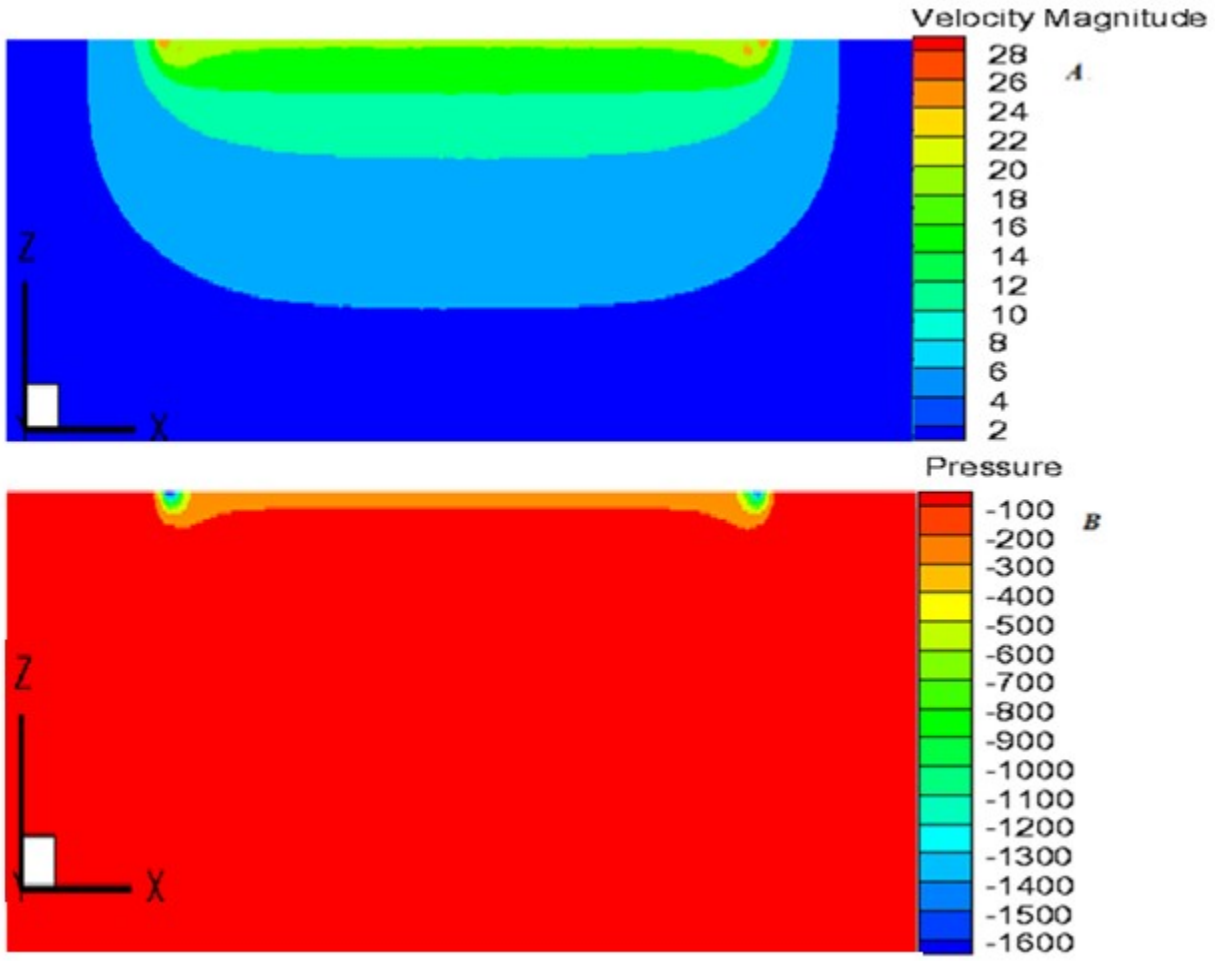

Figure 4: Distance from bottom 1 meter, plate x-z, A: velocity contour, B: pressure contour

Figure 5a shows the velocity profile on the y-z plane, where the velocity starts at 20 m/s in the center and reaches 30 m/s at the edges. This heterogeneity is related to the concentration of the flow at the edges and corners of the hood. In this case, a rapid decrease in the flow also occurs. Due to the smaller width of the hood compared to its length, more red areas are observed in this case, indicating high velocity at the corners of the hood.

Figure 5b shows the pressure distribution on the y-z plane. As can be observed, the pressure decreases in the center but reaches below 1500 Pa at the edges, which is associated with a high velocity of 30 m/s at the edges. The color pattern (red for positive pressure and blue for negative pressure) indicates a limited negative pressure that enhances the dispersion of pollutants.

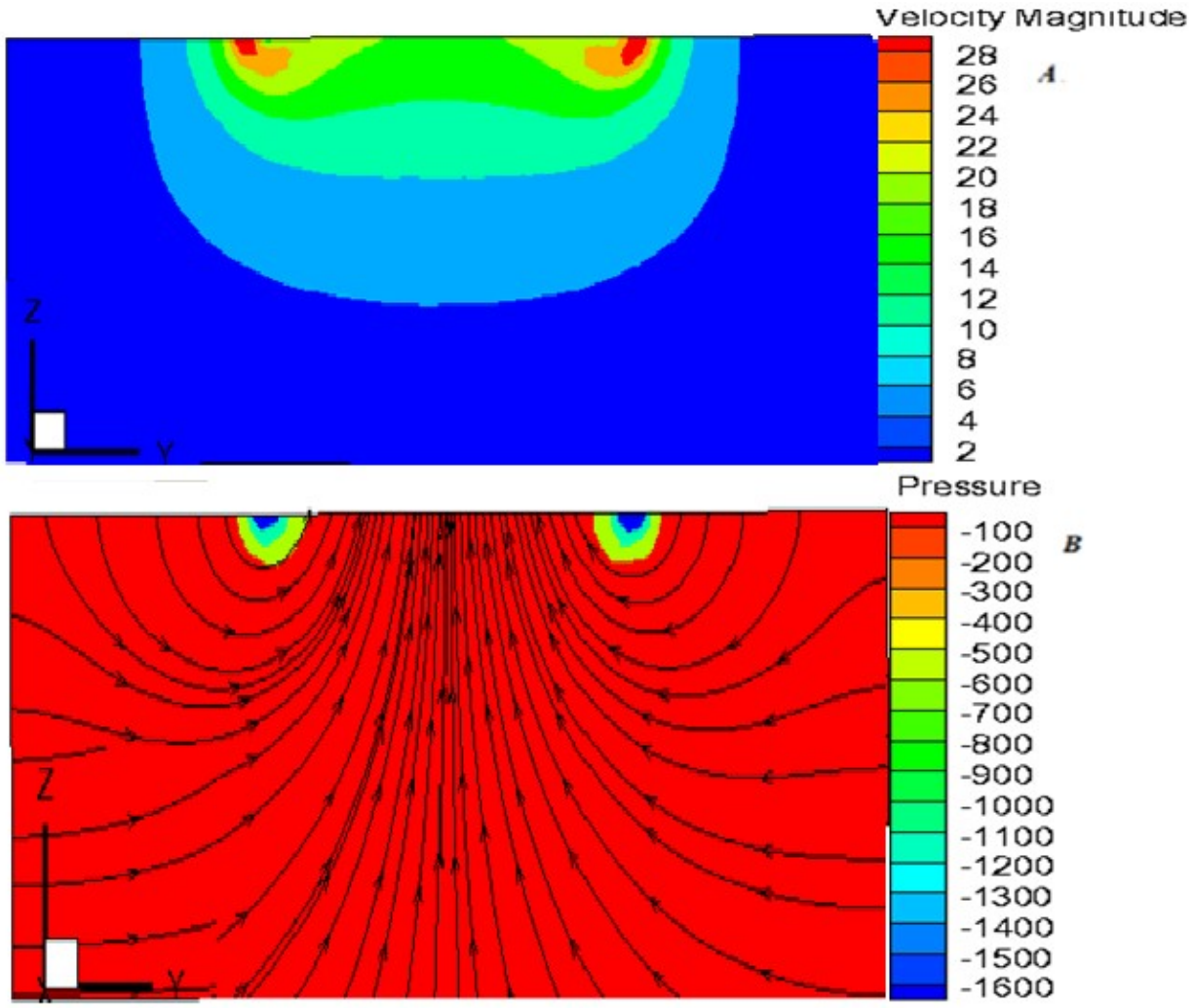

Figure 5: Distance from bottom 1 meter, plate y-z, A: velocity contour, B: pressure contour

3.1.2. Velocity and pressure contours when the hood is at a distance of 1.5 meters from the bottom

In Figure 6a, the velocity contour for the 1.5 m distance starts at 20 m/s and decreases more gently than in the 1 m case, which indicates a reduction in the wall effect. The velocity gradient in the x-z plane is moderate, indicating improved flow and fewer vortices compared to the 1 m case. In this case, suction improves compared to the 1 m case, but the wall effect remains strong.

Figure 6b shows that in the pressure contour for a distance of 1.5 m, the negative pressure at the inlet continues and approaches atmospheric pressure more smoothly, which is related to the greater distance from the bottom. The pressure gradient in the x-z plane is moderate, indicating a decrease in flow disturbance and an improvement in the pressure distribution. This contour shows that the pressure at the bottom of the plane approaches zero.

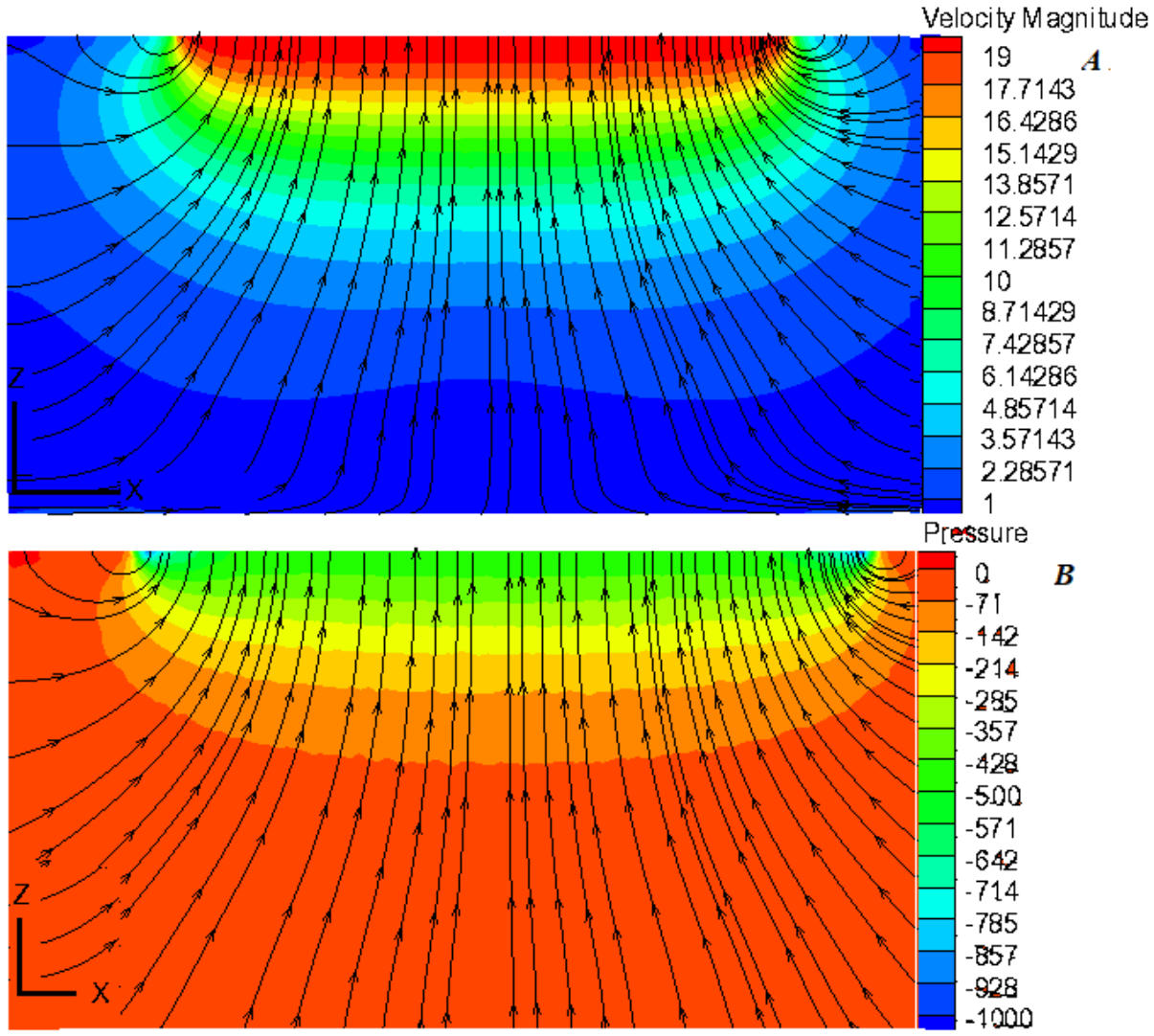

Figure 6: Distance from bottom 1.5 meters, plate x-z, A: velocity contour, B: pressure contour

Figure 7a shows the velocity distribution on the y-z plane. In the plane, the velocity in the center reaches 5 m/s. The suction range(capture zone) is slightly improved, but inhomogeneity is

observed at the corners. The color pattern indicates the expansion of the medium velocity region (green).

Figure 7b, which shows the pressure distribution on the y-z plane, shows that the pressure decreases in the center, but at the edges it drops below 1000 Pa, which is due to the high velocity at the edges. The color pattern indicates a wider negative pressure that reduces the dispersion. This improved pressure is consistent with the capture zone. The pressure contour shows a pressure of almost zero at the bottom.

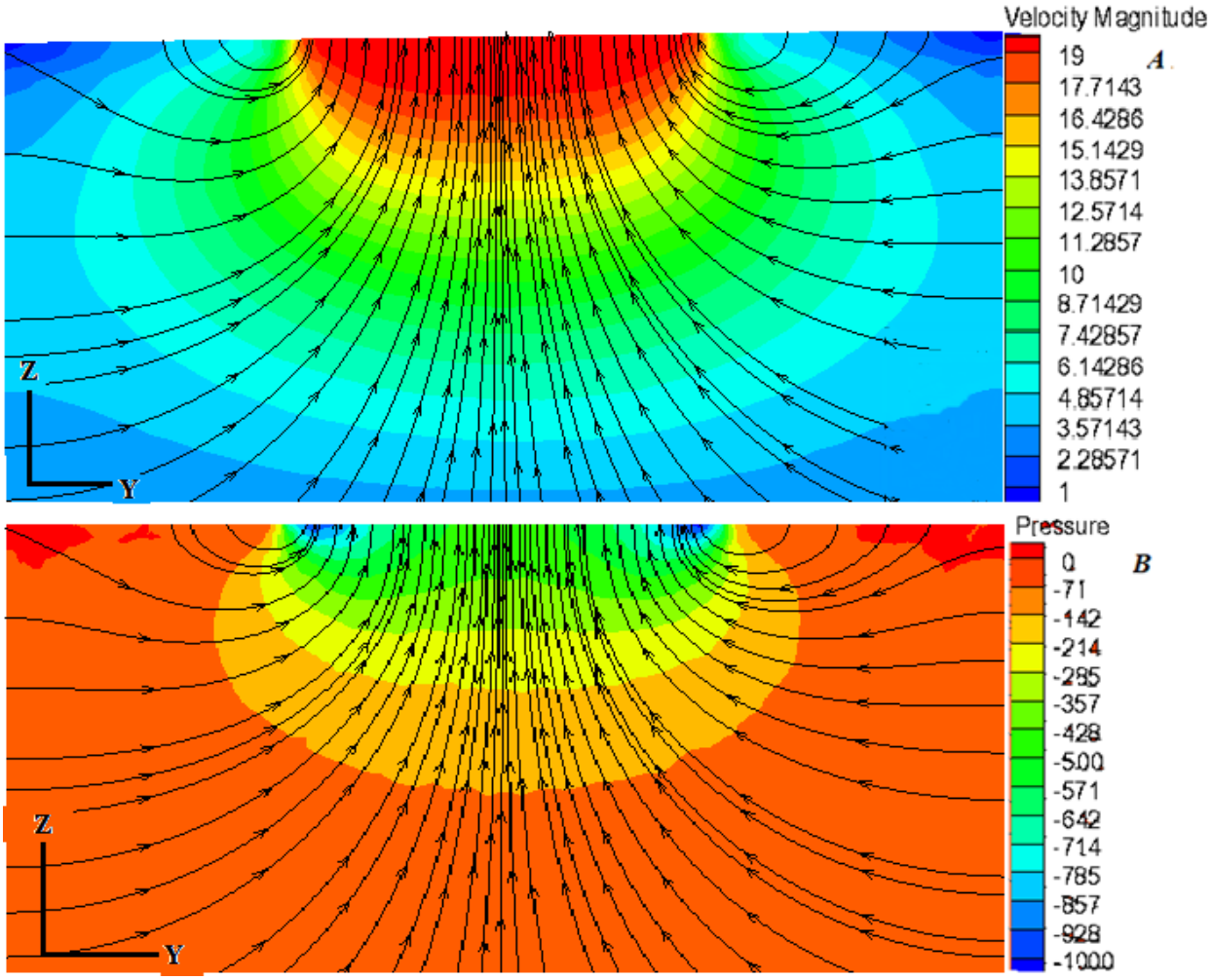

Figure 7: Distance from bottom 1.5 meters, plate y-z, A: velocity contour, B: pressure contour

3.1.3. Velocity and pressure contours when the hood is at a distance of 2 meters from the bottom

Figure 8a, which shows the velocity distribution on the x-z plane at 2 m, indicates that the velocity starts at 20 m/s and decreases uniformly, suggesting flow equilibrium and minimal wall

effect. The velocity gradient in the x-z plane is gentle, indicating stability and reduction of vortices. At some points in the corners of the hood, the velocity reaches about 32 m/s due to the formation of vortices.

Figure 8b shows that in the pressure contour for a distance of 2 m, the negative pressure at the inlet continues and uniformly approaches atmospheric pressure, which is related to the flow balance. The pressure gradient in the x-z plane is gentle, indicating an optimal pressure distribution and reduced disturbance. An acceptable negative pressure is also observed near the bottom.

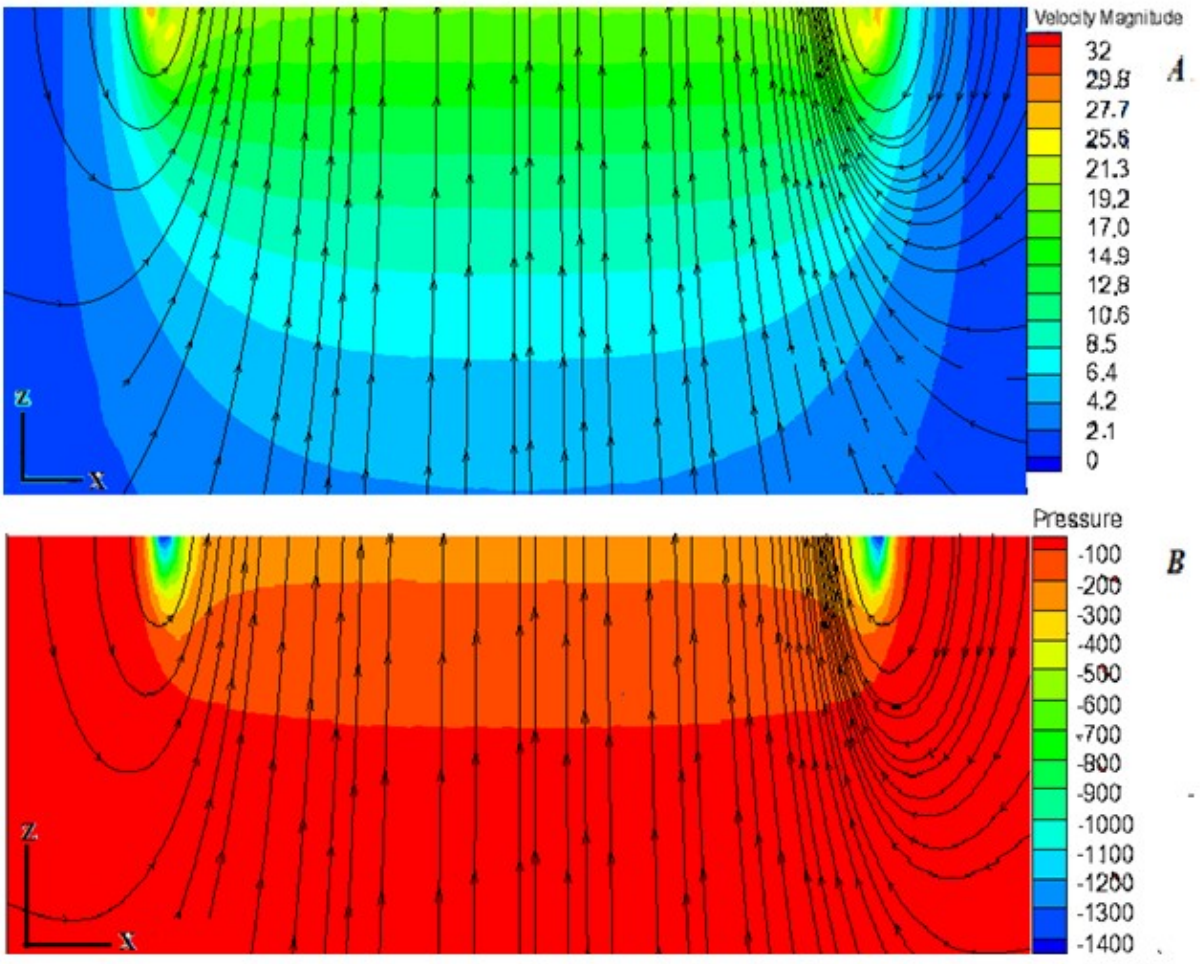

Figure 8: Distance from bottom 2 meters, plate x-z, A: velocity contour, B: pressure contour

In the y-z plane velocity distribution diagram in Figure 9a, the pressure decreases in the center but reaches 32 m/s at the edges, which is due to the flow concentration at the corners. The suction range(capture zone) is closest to the ACGIH standard, indicating optimal performance. The color pattern indicates equilibrium in the medium velocity region.

Figure 9b, which shows the pressure distribution on the y-z plane, indicates that the pressure decreases in the center but reaches -1400 Pa at the edges, corresponding to a low pressure and a velocity of 32 m/s at the edges. The color pattern indicates a balanced negative pressure that reduces dispersion. This pressure is consistent with the optimal range.

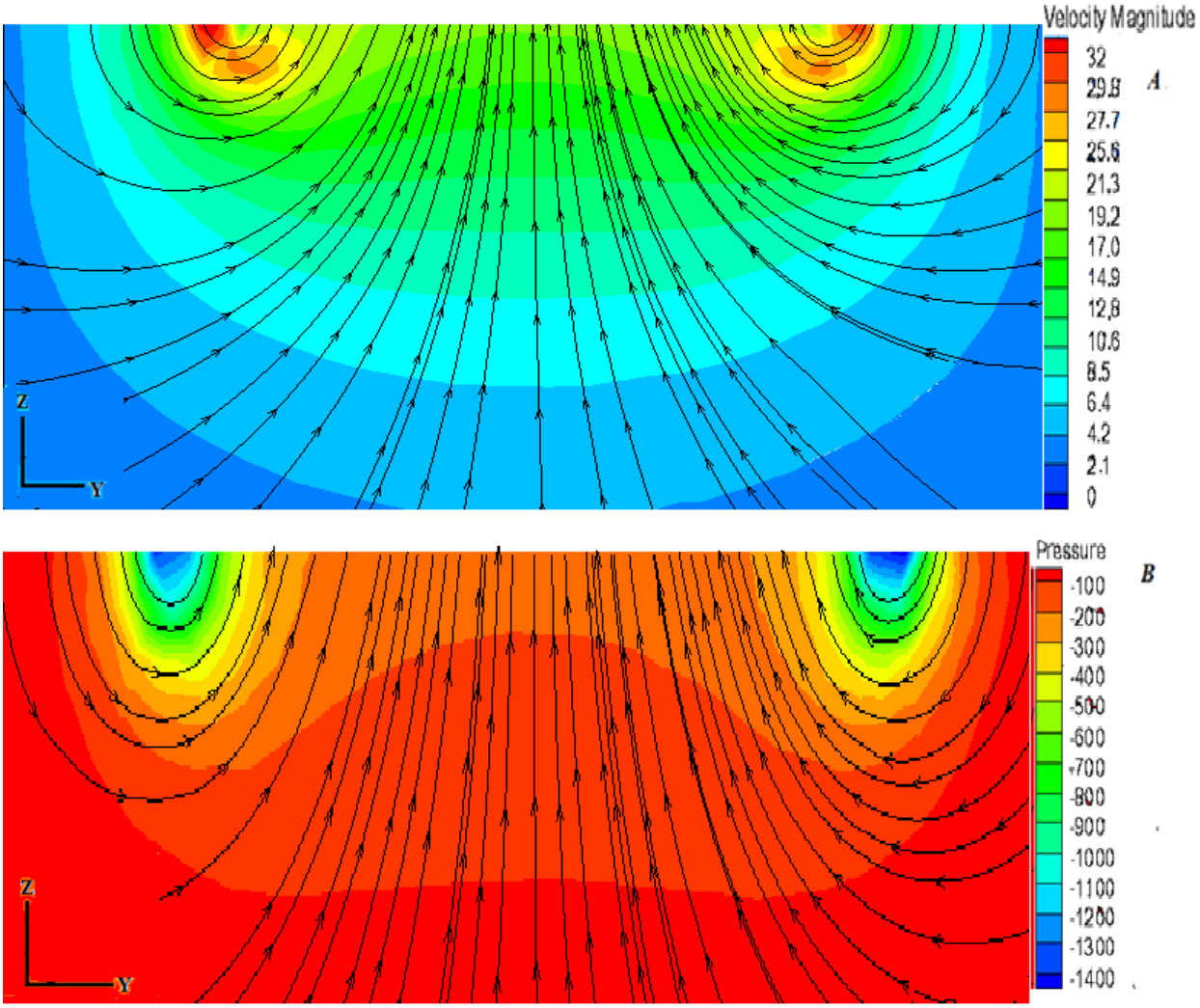

Figure 9: Distance from bottom 2 meters, plate y-z, A: velocity contour, B: pressure contour

3.1.4. Velocity and pressure contours when the hood is at a distance of 2.5 meters from the bottom

The velocity contour in Figure 10a, for a distance of 2.5 m, shows that the velocity starts at 20 m/s and decreases with oscillation, indicating dispersion of the flow at a further distance. The velocity gradient in the x-z plane is moderate with fluctuation, which means instability and reduced suction efficiency. The velocity at the corners of the hood also reaches 28 m/s, which indicates the flow separation and vortex formation at these points.

Figure 10b, which shows the pressure distribution on the x-z plane, shows that the negative pressure at the inlet continues and fluctuates towards atmospheric pressure, which is related to the flow dispersion. The pressure gradient on this plane is moderate with fluctuation, indicating an unbalanced pressure distribution and increased dispersion.

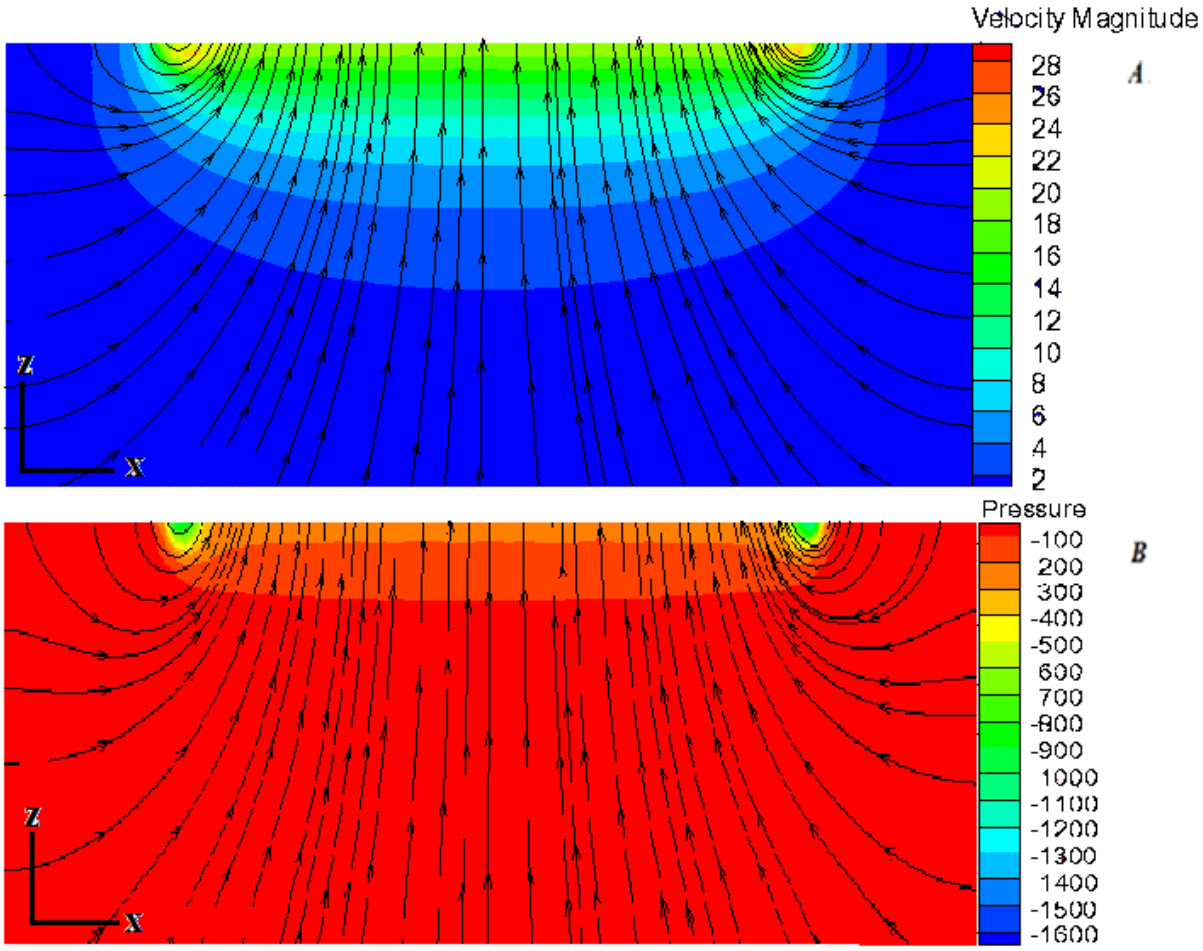

Figure 10: Distance from bottom 2.5 meters, plate x-z, A: velocity contour, B: pressure contour

Figure 11a shows the velocity distribution on the y-z plane. In this plane, the velocity gradually decreases from the center to the edges, reaching 28 m/s, which is related to the flow concentration at the corners. The velocity approaches zero at the upper part of the bottom, indicating a decrease in the suction amplitude.

Figure 11b is the pressure distribution on the y-z plane. In this plane, the pressure decreases in the center and reaches -1600 Pa at the edges, which corresponds to a velocity of 28 m/s. This unbalanced pressure is consistent with the suction amplitude in this case. The color pattern indicates a wide negative pressure with fluctuations that increase the dispersion.

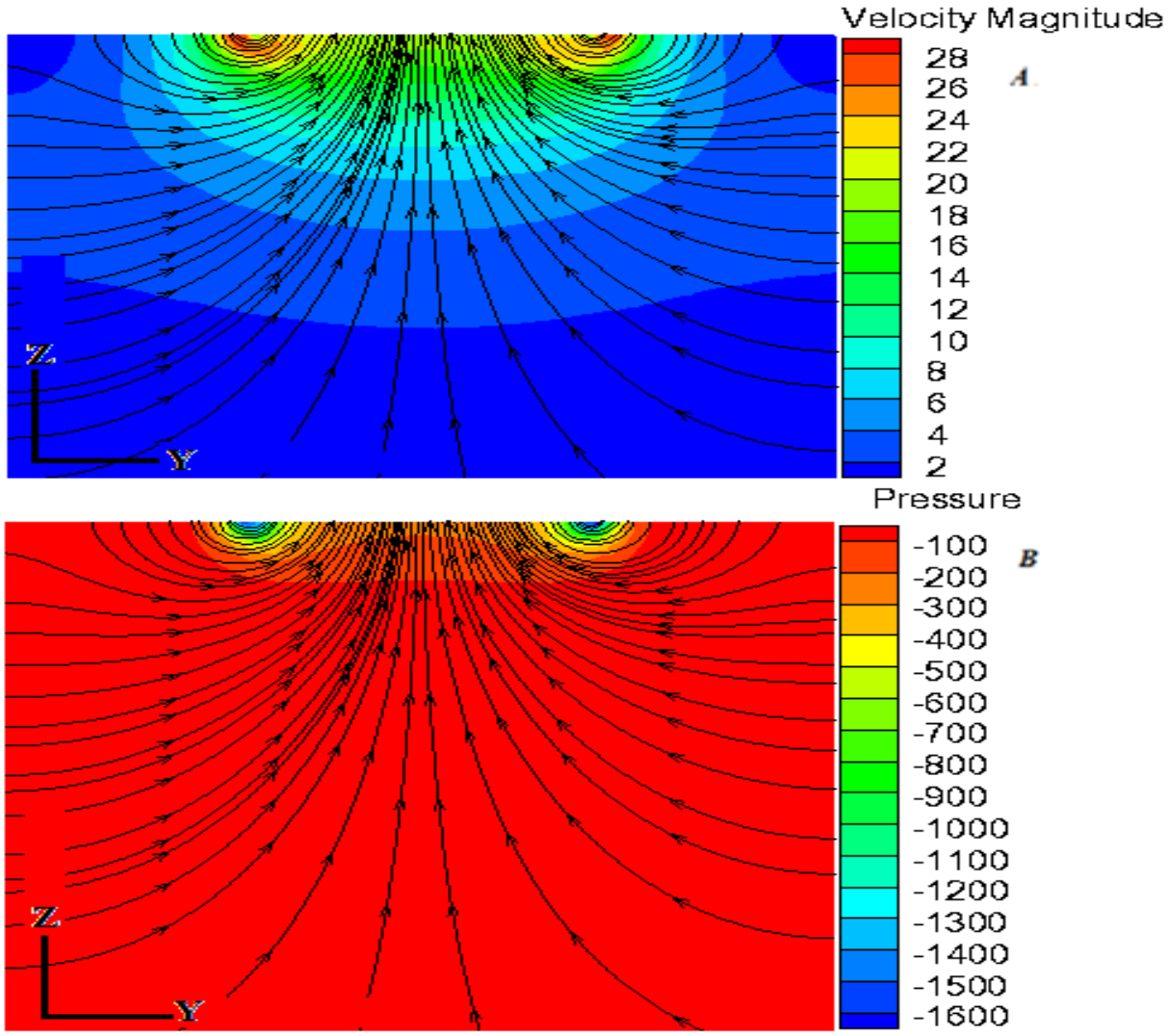

Figure 11: Distance from bottom 2.5 meters, plate y-z, A: velocity contour, B: pressure contour

3.1.5. Velocity and pressure contours when the hood is at a distance of 3 meters from the bottom

Figure 12a shows that the velocity starts at 20 m/s and decreases steadily, indicating that the flow is dispersed over a long distance. The velocity gradient in the x-z plane is gentle and steady, indicating relative stability but decreasing suction efficiency. The suction range (capture zone) is also low in this case. In this case, the velocity near the bottom is almost zero, indicating that the suction range is weak.

Figure 12b shows the pressure distribution on the x-z plane. The negative pressure at the inlet continues and gradually approaches atmospheric pressure, which is related to the flow dispersion. The pressure gradient in this plane is gentle and stable, indicating a stable but unbalanced pressure distribution. The red area, representing a pressure of -50 Pa, covers a large portion of the top of the wall, indicating that the suction in this area is low.

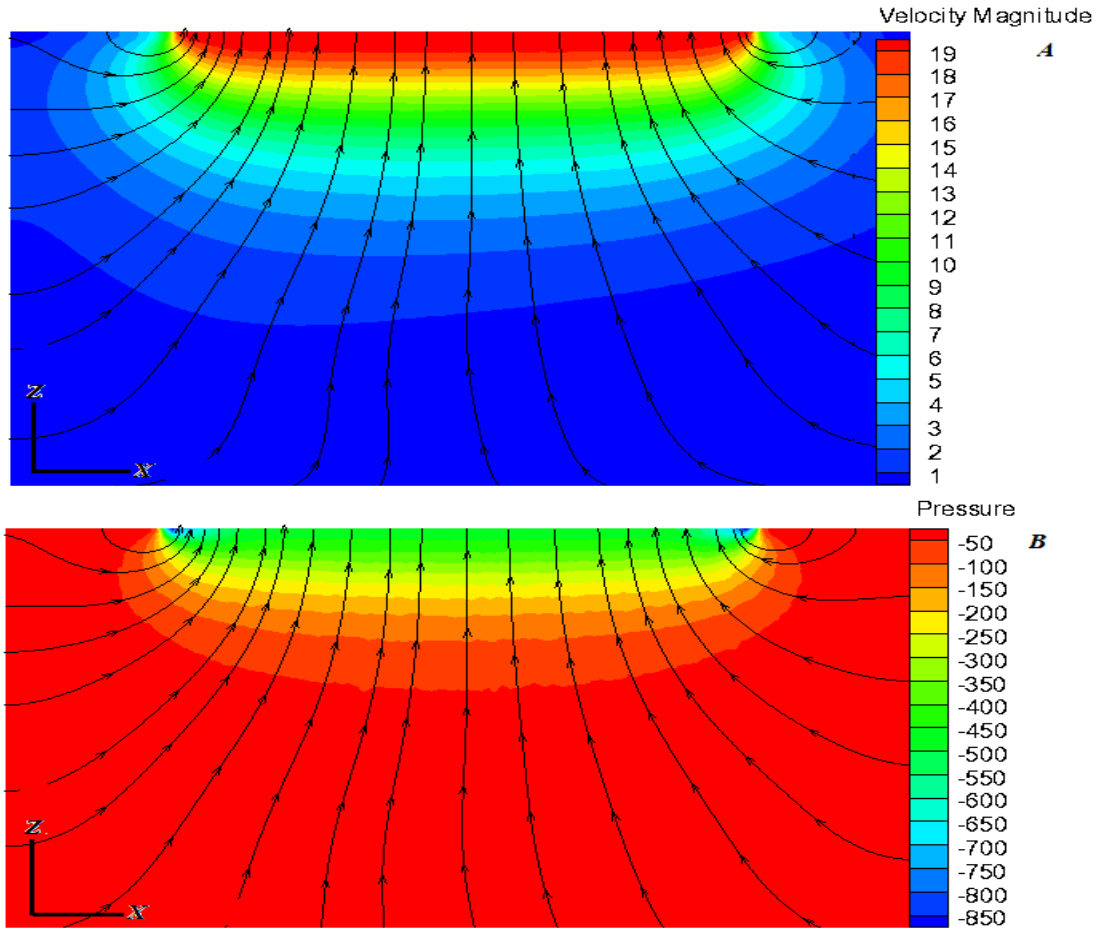

Figure 12: Distance from bottom 3 meters, plate x-z, A: velocity contour, B: pressure contour

As can be seen in Figure 13a, in the y-z plane, the velocity at the center reaches 1 m/s, but at the edges, the velocity increases, which indicates that the inhomogeneity in the velocity points to the flow concentration. The suction range in this case is low and needs to be improved. The color pattern indicates a wide average velocity region (green) that increases the dispersion. The low velocity near the wall indicates low suction in this case.

Figure 13b, which shows the pressure distribution on the y-z plane, shows that the pressure decreases in the center and reaches a value of -1000 Pa at the edges, which is related to the high velocity at the corners of the hood and the flow separation in that area. The color pattern indicates a stable, widespread negative pressure that increases the dispersion. This stable pressure is consistent with the suction range (capture zone) in this case. The area above the wall has very little negative pressure, indicating a low suction range in this case.

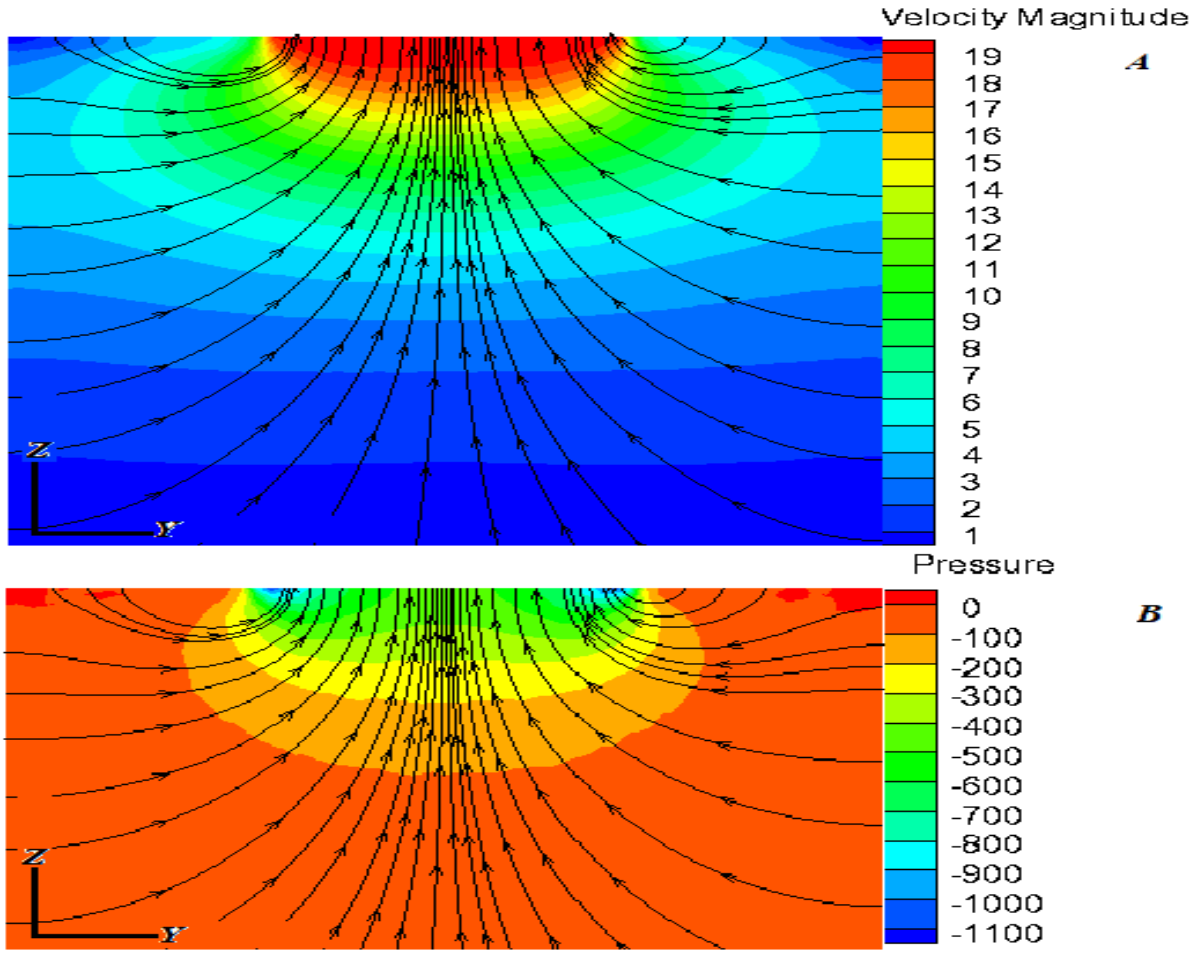

Figure 13: Distance from bottom 3 meters, plate y-z, A: velocity contour, B: pressure contour

3.2. Analyzing the velocity profile on the hood centerline

Figure 14a shows an imaginary line drawn from the center of the hood to the bottom. Figure 14b shows the velocity distribution diagram on the imaginary line connecting the center of the hood to the bottom, for different distances.

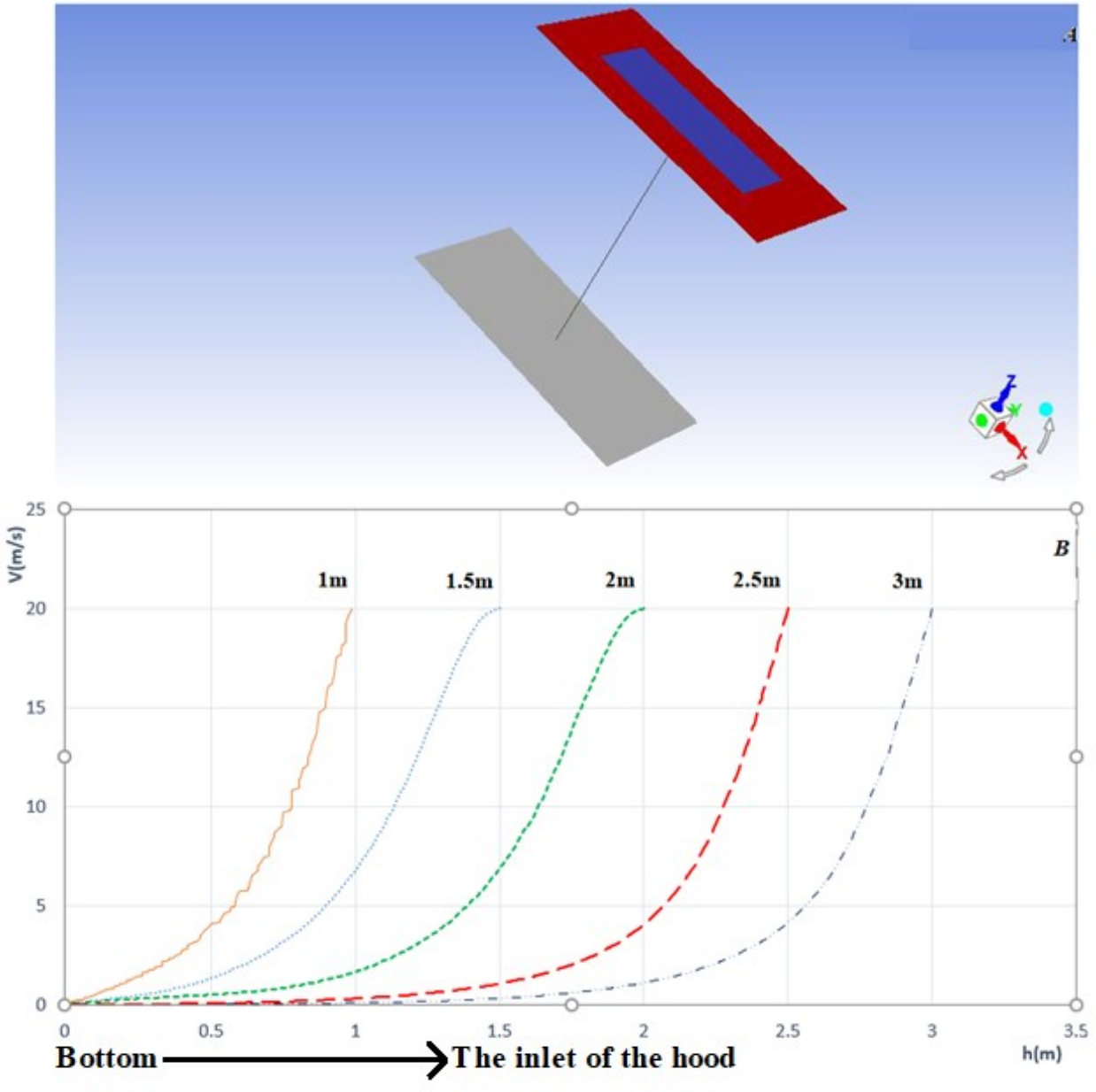

Figure 14: A: The imaginary line drawn from the center of the hood to the bottom. B: The velocity distribution diagram on the imaginary line connecting the center of the hood to the bottom

At a distance of 1 meter from the bottom, the velocity starts at 20 m/s and decreases very rapidly. A high gradient indicates weak suction and a strong wall effect. The weak amplitude is due to the flow being compressed by the wall. This is not suitable for applications close to the bottom.

For a distance of 1.5 meters from the bottom, the velocity starts at 20 m/s and decreases more gently than at 1 meter. The suction range is also improved, but is still below. The fluctuations in the graph are consistent with the fluctuations in the velocity contour in the x-z plane.

At a distance of 2 meters from the bottom, we have a uniform decrease in velocity in this case. The suction range (capture zone) in this case is the best and is close to the theoretical value. As can be seen in the diagram, it performs best near the wall.

For a distance of 2.5 meters, the velocity starts at 20 m/s and gradually decreases. The velocity decreases gently and with fluctuations. There is very little suction at the top of the wall due to the low velocity.

At a distance of 3 meters from the bottom, the velocity starts at 20 m/s and gradually decreases. The velocity decreases gently and steadily. The velocity reaches zero at a much higher range from the bottom, which leads to a decrease in the suction range.

3.3. Validation

3.3.1. Capture Velocity

According to ACGIH (American Conference of Governmental Industrial Hygienists) guidelines, Capture Velocity is the air velocity that must exist at a given point in front of the hood opening or at the point of emission of the pollutant for the pollutant particles, vapors, or gases to be drawn into the hood and into the ventilation system. This velocity must be sufficient to overcome environmental disturbances (such as thermal convection, general ventilation, and human movement) and prevent the pollutants from entering the respiratory zone.

3.3.2. Capture Zone

According to the ACGIH guidelines, the hood suction speed is calculated with the following approximate equation:

$$V = \frac{Q}{A + 10X^2}$$

(7)

In this equation, **Q** is the flow rate (m^3/s), **A** is the hood area (m^2), and **X** is the distance from the hood opening (m). The distance at which the hood suction speed reaches the minimum effective value is defined as the hood's capture zone. According to the ACGIH standard, this value is defined as 0.5 m/s.

In this study, we have a hood with dimensions of 0.65 × 1.5 m, resulting in a hood area of 0.975 m^2. Considering that the velocity at the center of the hood is 20 m/s, the flow rate is 19.5 m/s.

According to equation 7, for a critical velocity of 0.5 m/s, the capture zone is 1.95 m, which means that the suction range of the hood in an ideal state, without considering the floor effect, is approximately 1.95 m.

According to the results obtained by CFD in the velocity profile in Figure 13b at different distances from the hood, the capture zone (the distance where the velocity reaches 0.5 m/s) is shown in Table 1. Therefore, in the case where the distance of the hood from the floor is 2 meters, we observe a uniform decrease in velocity to 0.5 m/s, and with a suction range of 1.715 meters, the best result is obtained, which is close to 1.95 meters, which is the same as the ACGIH number. The velocity contour at this distance shows a uniform gradient in the longitudinal and transverse planes, but in the corners of the hood, high velocity is observed due to flow separation. The pressure contours also show a suitable negative pressure.

Table 1: Capture zone gained by CFD

Location of the hood (Distance from the bottom) (m)	Capture zone (m)
1	**0.894**
1.5	**1.242**
2	**1.715**
2.5	**1.320**
3	**1.328**

4. Discussion and conclusion

A complete study was conducted on the range of effects of industrial hoods under isothermal conditions, and the results were verified using the ACGIH standard. A distance of 2 meters yields the best performance, with a suction range of 1.715 m. Distances of 1 meter and 1.5 meters are not acceptable due to the wall effect, and distances of 2.5 meters and 3 meters are not acceptable due to the reduction of the capture zone(suction range). In all cases, vortices form in the corners of the hood due to flow concentration and separation; at these points, the pressure is sharply reduced, and the velocity exceeds 20 m/s.

Symbols used

Greek letters

ρ	Density [kg m^{-3}]
ε	Turbulence lost rate m^2s^{-2}
u	Velocity [m s^{-1}]
μ	Dynamic viscosity [Pa s]
τ	Tension tensor
∇	divergence
$(\nabla u)^T$	$\nabla(\nabla \cdot u)$
μ_t	Turbulent viscosity [Pa s]
σ_k	k-ε model coefficient
σ_ε	k-ε model coefficient
$C1\varepsilon$	k-ε model coefficient
$C2\varepsilon$	k-ε model coefficient
C_μ	k-ε model coefficient

Abbreviations

ACGIH	American Conference of Governmental Industrial Hygienists
A	Area of hood [m^2]
g	Gravitational acceleration [~ 9.8 m s^{-2}]
F	Other volumetric forces [N/m^3]
I	Conservation of momentum and the effects of pressure, viscosity, and external forces
k	Kinetic energy of turbulence [m^2s^{-2}]
P	Pressure [Pa]
P-k	Turbulence kinetic energy production
Q	Volumetric flow rate [m^3s^{-1}]
x	Distance from Hood Inlet [m]
V	Velocity of flow [ms^{-1}]
x	Coordinate position
y	Coordinate position
z	Coordinate position

References

[1] ACGIH. (2016). Industrial ventilation: A manual of recommended practice for design. (Report on the control of pollutants by industrial hoods).

[2] Flynn, M., & Ljungqvist, B. (1995). Impact of airflow rate and hood distance on suction efficiency. Journal of Industrial Hygiene, 45(3), 123-130.

[3] Launder, B. E., & Spalding, D. B. (1974). The numerical computation of turbulent flows. Computer Methods in Applied Mechanics and Engineering, 3(2), 269-289.

[4] Wilcox, D. C. (1998). Turbulence modeling for CFD (Evaluation of the Realizable k-ε model accuracy in complex flows). DCW Industries.

[5] Zhang, Z., & Chen, Q. (2012). Comparison of the accuracy of CFD simulations and experimental measurements with a focus on fine meshing. Building and Environment, 47, 245-253.

[6] Safarzadeh, A., & colleagues. (2010). Expansion of suction range and pollutant dispersion in industrial hoods. Environmental Science & Technology, 44(12), 4567-4573.

[7] Zhang, Z., & Chen, Q. (2012). Comparison of the accuracy of CFD simulations and experimental measurements with a focus on fine meshing. Building and Environment, 47, 245-253.

[8] Zhao, Y., Li, A., Tao, P., & Gao, R. (2013, June). The impact of various hood shapes, side panels, and exhaust duct arrangements on the performance of typical Chinese-style cooking hoods. In *Building Simulation* (Vol. 6, No. 2, pp. 139-149). Tsinghua Press.

[9] Huang, Y., Wang, Y., Ren, X., Yang, Y., Gao, J., & Zou, Y. (2016). Ventilation guidelines for controlling smoke, dust, droplets, and waste heat: Four representative case studies in Chinese industrial buildings. *Energy and Buildings*, *128*, 834-844.

[10] Logachev, K. I., Ziganshin, A. M., & Averkova, O. A. (2018). Simulations of dust dynamics around a cone hood in updraft conditions. *Journal of Occupational and Environmental Hygiene*, *15*(10), 715-731.

[11] Logachev, K. I., Ziganshin, A. M., & Averkova, O. A. (2019). On the resistance of a round exhaust hood, shaped by the outlines of the vortex zones occurring at its inlet. *Building and Environment*, *151*, 338-347.

[12] Zhang, J., Wang, J., Gao, J., Cao, C., Lv, L., Xie, M., & Zeng, L. (2020). Critical velocity of active air jet required to enhance free opening rectangular exhaust hood. *Energy and Buildings*, *225*, 110316.

[13] Kim, J., & Lee, H. (2020). Validation of CFD simulation results with ACGIH standards in industrial ventilation. International Journal of Ventilation, 19(3), 189-198.

[14] Liu, Y., Xia, T., Wang, Y., Chen, J., & Li, X. (2020). Simulation and experimental investigation of dust-collecting performances of different dust exhaust hoods. *Journal of the Air & Waste Management Association*, *70*(12), 1367-1377.

[15] Li, X., Jiang, Y., Zhu, J., Wang, L., Zhang, M., Xu, X., ... & Cao, Y. (2021). Air curtain dust-collecting technology: Investigation of industrial application in a tobacco factory of the air curtain dust-collecting system. *Process Safety and Environmental Protection*, *149*, 676-683.

[16] Logachev, K. I., Ziganshin, A. M., Popov, E. N., Averkova, O. A., Kryukova, O. S., & Gol'tsov, A. B. (2021). An experiment determining pressure loss reduction using a shaped round exhaust hood. *Building and Environment*, *190*, 107572.

[17] Song, Y., Chen, X., Zhang, Z., Cao, S., Du, T., & Guo, H. (2022). Studies on the control of kitchen pollutants by an exhaust hood with air-filled slots. *Journal of Building Engineering*, *48*, 103891.

[18] Abbasnia, S., Shafieyoun, V., Golzarijalal, M. and Nasri, Z., 2021. Computational fluid dynamics versus experiment: an investigation on liquid weeping of Nye Trays. *Chemical Engineering & Technology*, *44*(1), pp.6-14.

[19] Abbasnia, S., Yu, Q. J., Nasri, Z., & Khojasteh, A. (2022). Nye tray versus sieve tray: Experimental study on hydrodynamic parameters. *Chemical Engineering & Technology*, *45*(1), 110-118.

[20] Abbasnia, S., Nasri, Z., & Najafi, M. (2019). Comparison of the mass transfer and efficiency of Nye tray and sieve tray by computational fluid dynamics. *Separation and Purification Technology*, *215*, 276-286.

[21] Abbasnia, S., & Abbasnia, A. A. Computational fluid dynamics comparison of two-equation turbulence models by studying hydrodynamic parameters in the distillation trays.

[22] Abbasnia, S., & Abbasnia, A. Simulation of a turbine flow meter with a cylindrical support fence using CFD.

[23] Abbasnia, S., Nasri, Z., Shafieyoun, V., & Golzarijalal, M. (2021). Nye tray vs sieve tray: A comparison based on computational fluid dynamics and tray efficiency. *The Canadian Journal of Chemical Engineering*, *99*, S681-S692.

[24] ABBASNIA, S., Shafieyoun, V., & Nasri, Z. (2020). CFD versus experiment: an investigation on liquid weeping of Nye tray. *Authorea Preprints*.